Bioresource Technology 285 (2019) 121325

Contents lists available at ScienceDirect

Bioresource Technology

journal homepage: www.elsevier.com/locate/biortech

Torrefaction and carbonization of refuse derived fuel: Char characterization and evaluation of gaseous and liquid emissions

Catarina Nobre[a], Octávio Alves[a,b], Andrei Longo[a], Cândida Vilarinho[c], Margarida Gonçalves[a,b,*]

[a] MEtRICs, Mechanical Engineering and Resource Sustainability Center, Department of Sciences and Technology of Biomass, Faculty of Sciences and Technology, NOVA University of Lisbon, 2829-516 Caparica, Portugal

[b] VALORIZA, Research Center for Endogenous Resource Valorization, Polytechnic Institute of Portalegre, 7300-555 Portalegre, Portugal

[c] MEtRICs, Mechanical Engineering and Resource Sustainability Center, Mechanical Engineering Department, School of Engineering, University of Minho, 4804-533 Guimarães, Portugal

ARTICLE INFO

Keywords:
Refuse Derived Fuel (RDF)
Lignocellulosic wastes
Torrefaction
Carbonization
Liquid emissions

ABSTRACT

Refuse derived fuel containing non-hazardous industrial wastes was subjected to torrefaction and carbonization in an industrial furnace. The RDF samples were heated at 300 °C and 400 °C, for 30 min, yielding solid products (chars) as well as gases and liquids. Proximate and ultimate composition, mineral composition, chlorine content and high heating value were determined for the original sample and the produced chars. Thermal treatment produced RDF chars with carbon contents of 61.6 and 80.2 wt%, and high heating values of 19.9 and 23.5 MJ/kg, that could be further upgraded by washing with water to reduce ash and chlorine concentrations and improve calorific value. Gas products were composed of carbon dioxide and carbon monoxide with minor amounts of hydrogen. Methane was only detected in the gas produced at 400 °C. The process generated liquid products rich in organic compounds that represent potential in further energy or material recovery.

1. Introduction

Wastes are overflowing by-products of all human activities and their sustainable management is a major concern of present society. Waste generation can be related to several environmental problems, namely greenhouse gas emissions or water pollution. Global generation of municipal solid wastes (MSW) is around 1.4 billion tons per year, with a projected increase to 2.2 billion tons in 2025 (Anthraper et al., 2018) and 9.5 billion tons by 2050 (Beyene et al., 2018). Owing to their large availability and continued production, wastes may contribute greatly to energy provision and secondary resource recovery (Astrup et al., 2014).

Waste-to-Energy (WtE) systems are sustainable waste management solutions aiming to reduce landfill deposition and fossil fuel consumption, by valorization of solid wastes that contain non-recyclable materials and have high energy contents. One of the ways to effectively reuse waste as an energy vehicle is to convert it to Refuse Derived Fuel (RDF) or Solid Recovery Fuel (SRF) (Białowiec et al., 2017). These are waste-derived fuels obtained by treatment of non-hazardous wastes such as MSW, regular industrial wastes (RIW), construction and demolition wastes (CDW) or sludge from water or wastewater treatment plants. SRF refers to a solid fuel that results from the treatment of waste materials and meets the classification and specification requirements laid down by CEN/TS 15359:2009, for energy recovery in incineration and co-incineration plants (Rada and Andreottola, 2012). On the other hand, RDF is a broader designation used to label waste-derived fuels that may not obey specific technical characteristics and are therefore considered of lower quality (Nasrullah et al., 2015). The RDF production process is considered a priority solution in industrialized countries (Dalai et al., 2009). It allows significant reductions on the amount of end-of-life materials sent to landfills and it enhances the energy recovery from different wastes. The production of these fuels aims to improve the heating value and homogenize particle size of the corresponding raw materials that include plastics, rubbers, packages, textiles, lignocellulosic wastes, among others (Białowiec et al., 2017; Dalai et al., 2009).

Although RDF and SRF have improved fuel properties when compared to the original wastes, their application in thermochemical conversion systems is often hindered by their heterogeneous composition, low grindability and poor fuel properties, such as low calorific value, high moisture, ash and chlorine contents (Edo et al., 2017). Fuels with significant chlorine and ash contents are known to cause several operational issues, including slagging, fouling, boiler corrosion and

* Corresponding author at: Department of Science and Technology of Biomass, Faculty of Sciences and Technology, NOVA University of Lisbon, 2829-516 Caparica, Portugal.
E-mail address: mmpg@fct.unl.pt (M. Gonçalves).

https://doi.org/10.1016/j.biortech.2019.121325
Received 1 February 2019; Received in revised form 4 April 2019; Accepted 5 April 2019
Available online 06 April 2019
0960-8524/

problematic emissions such as hydrochloric acid or dioxins/dibenzofurans (PCDD/Fs) (Chyang et al., 2010; Silva et al., 2014). RDF with large polymeric fractions may create problems of clogging in the feeding systems and promote char accumulation in combustion or gasification beds. Polymers like PE (polyethylene) or PS (polystyrene), that are usually found in RDF, are recalcitrant to thermal decomposition, typically decomposing in a temperature range between 350 °C and 500 °C (Fellner et al., 2011; López et al., 2011), whereas lignocellulosic materials start their decomposition at around 225 °C (Prins et al., 2006a). On account of these challenging issues, there is a need to explore RDF fuel upgrading in order to further improve fuel quality and reach a widespread and sustainable use of this fuel.

Thermochemical upgrading operations such as torrefaction and carbonization have been extensively applied to different biomass feedstocks such as corn stalk, wood wastes, spent coffee grounds or microalgae waste, yielding homogeneous biochars with lower moisture content, higher calorific values, lower O/C ratios, higher hydrophobicity and enhanced grindability when compared with the original biomasses (Chen et al., 2018a; Wilk et al., 2016; Zhang et al., 2018). In the torrefaction process, organic matter is heated with little or no oxygen, usually at atmospheric pressure, in a temperature range between 200 and 300 °C (Verhoeff et al., 2011). Carbonization occurs in similar conditions but at higher temperatures (300–500 °C) (Qi et al., 2018). In both processes, the main product is a char that presents a homogeneous carbon structure and contains some inert mineral components. In addition to the char, gas products (primarily carbon dioxide, carbon monoxide and methane) and a condensable liquid (water, acetic acid and other oxygenated compounds) are also produced (Tumuluru et al., 2011). The amount of each product is dependent on the process main parameters, namely temperature, heating rate or residence time, as well as on the characteristics of the feedstock (Tumuluru et al., 2011; van der Stelt et al., 2011; Volpe et al., 2015). Biomass is by far the most used raw material in torrefaction and carbonization applications. There are less studies focused on the torrefaction or carbonization of other waste streams, such as MSW or RDF, and the majority of those is dedicated to the characterization of the main product (char) and does not include the characterization of the corresponding emissions (gas product and condensates). The characterization of the emissions associated with torrefaction or carbonization is necessary to develop appropriate strategies to treat or reduce emissions and therefore improve the sustainability of those processes at an industrial scale. Detailed description of gaseous and/or liquid emissions associated with these thermal conversion processes has been done mostly for biomass feedstocks, such as rice husk (Chen et al., 2018b), bamboo (Chen et al., 2015) or sorghum (Yue et al., 2017).

Yuan et al. (2015) tested the torrefaction of MSW components at temperatures from 250 °C to 450 °C, under a N_2 atmosphere, using a residence time of 30 min. The MSW chars showed increased grindability and a significant chlorine reduction while their high heating values (HHV) were improved in the temperature range from 250 °C to 350 °C, reaching a value of 29.6 MJ/kg at 300 °C.

RDF torrefaction was tested by Białowiec et al. (2017) at temperatures in the range of 200–300 °C and a residence time of 1 h. The process caused a 21.5% mass reduction essentially due to the elimination of moisture and volatile components. The authors state that the carbonized RDF showed higher homogeneity and its lower heating value (LHV) increased, relatively to the original RDF, from 19.6 to 25.3 MJ/kg.

Haykiri-Acma et al. (2017) investigated the properties of RDF chars obtained by carbonization at temperatures from 400 °C to 900 °C. According to this work, increasing the carbonization temperature within this range led to an increase in the ash content of the produced chars, as well as a decrease in their volatile matter and fixed carbon contents. These composition changes negatively impacted the high heating value of the chars, thus the authors concluded that RDF carbonization should not be done in temperatures above 400 °C, because only at lower temperatures it is possible to obtain a significant increase in fixed carbon and therefore an increase in the calorific value of the RDF chars.

Edo et al. (2017) evaluated the torrefaction of different wastes, including MSW and RDF and studied the combustion of the resulting torrefaction gas. In particular, the authors showed that torrefaction enabled a partial elimination of organic chlorine present in the raw materials, thus producing chars with a lower tendency to originate hazardous chlorinated compounds.

The results obtained by the authors mentioned above indicate that both torrefaction and carbonization are viable pathways to upgrade RDF but the choice of the temperature operating range will mainly depend on the RDF initial composition (Białowiec et al., 2017; Edo et al., 2017; Haykiri-Acma et al., 2017; Yuan et al., 2015). Given the higher chemical stability of polymeric materials the higher the concentration of those materials in a given RDF sample the higher should be the upgrading temperature used in its treatment (Nobre et al., 2019).

Most literature reports on RDF torrefaction or carbonization were performed in the sub-kilogram scale (Białowiec et al., 2017; Edo et al., 2017; Haykiri-Acma et al., 2017), but given the heterogeneity of RDF the evaluation of these treatments in a larger scale could probably provide more representative information on product composition. Recari et al. (2017) studied torrefaction of SRF in a continuous reactor, at a 13 kg/h rate, processing around 3.3 kg of material in each test, but did not study the associated emissions.

In this work, the thermochemical upgrading of an industrial refuse derived fuel (RDF) containing comparable amounts of lignocellulosic and polymeric components, was studied at temperatures corresponding to the higher limit of the torrefaction range (300 °C) and an average temperature in the carbonization range (400 °C). For temperatures lower than 300 °C, a poor decomposition of the polymeric fraction can be expected, while for temperatures above 400 °C, substantial loss of fixed carbon may hinder mass and energy yields (Haykiri-Acma et al., 2017). The tests were performed at a pre-pilot scale (5 kg samples), in order to achieve a representative evaluation of the conversion process and associated emissions. The RDF chars as well as the co-produced gases and condensates were characterized and the mass and energy yields were evaluated in order to discuss the process performance and the possible pathways for valorization or remediation of the secondary products.

2. Materials and methods

2.1. Raw material

The RDF sample used in this work was produced from non-hazardous industrial wastes and was supplied by CITRI S.A., a Portuguese waste management company. Sampling of the RDF was performed through quartering, starting with a lot size of 100 kg, and ending with a gross sample of 25 kg. The gross sample had an average particle diameter between 30 and 80 mm. Main components of the sample were determined by manual sorting, through three sub-samples of 1 kg. The RDF sample was composed by plastics (22.9 ± 1.2 wt%), wood (5.0 ± 0.4 wt%), paper and cardboard (17.9 ± 3.9 wt%), foam (0.7 ± 0.0 wt%), textiles (7.9 ± 1.8 wt%), glass (0.2 ± 0.0 wt%), aluminum (0.5 ± 0.0 wt%) and miscellaneous particles with diameter > 500 μm (39.9 ± 3.9 wt%), ≥250 μm (2.6 ± 0.5 wt%) and < 250 μm (2.4 ± 0.1 wt%).

2.2. Torrefaction and carbonization tests

RDF was subjected to torrefaction and carbonization at the temperatures of 300 °C and 400 °C, respectively, using an industrial rotary furnace (MJ Amaral, model FR 100), equipped with an emissions collection system schematically represented in Fig. 1. For each run, approximately 5 kg of RDF (as received) were placed in the furnace, the air was removed using a vacuum pump (in order to reduce oxygen

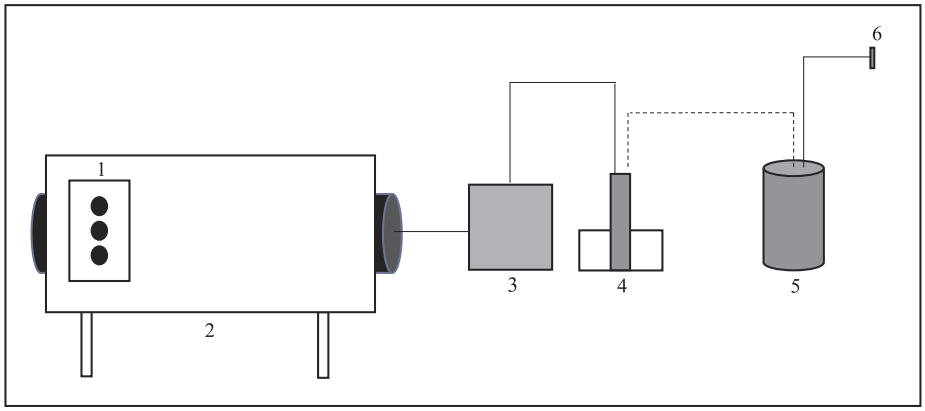

Fig. 1. Schematic representation of the carbonization system used in this work. Legend: 1 – Control panel; 2 – Rotary pyrolysis furnace; 3 – Condensation chamber (1st collection point); 4 – Condensation chamber (2nd collection point); 5 – Water column; 6 – Gas collection.

availability), and the rotation movement was initiated at a rate of 1 rpm. The furnace was then heated to 200 °C for 15 min, to allow for temperature equilibration with the furnace walls and reduction of the RDF sample moisture. Afterwards, temperature was risen to 300 °C or 400 °C, at 4 °C/min and held at those values for 30 min. During this period pressure increased as gas products were continuously formed and released through two condensation chambers and a water scrubbing column before being vented to atmosphere. The condensed phases collected in the condensation chambers (1st and 2nd collection points) were recovered in the end of each test and kept at 4 °C until analysis. Non-condensable gases were collected in 5 L Tedlar bags for later characterization.

2.3. Refuse derived fuel and refuse derived fuel char characterization

Before analytical characterization, the RDF gross sample was air-dried for 15 days, and homogenized using a mechanical mill (DeLonghi mill). The homogenized RDF samples were stored in plastic containers until analysis. The RDF char samples obtained in each test were milled and sieved to a particle diameter < 500 μm (Retsch sieve) and stored in glass containers until analysis. All analytical determinations were done in triplicate and results are presented as average values with corresponding standard deviations.

Moisture, volatile matter and ash contents were determined according to CEN/TS 15414-3:2010, EN 15402:2011 and EN 15403:2011, respectively. Fixed carbon content was obtained by difference, on a dry basis. Ultimate analysis (carbon, hydrogen, nitrogen and sulfur) was performed using an elemental analyzer (Thermo Finnigan – CE Instruments Model Flash EA 112 CHNS series). Oxygen content was calculated by difference, on a dry ash-free basis. High heating values (HHV) of the RDF and the RDF char samples were determined with a calorimeter bomb (IKA C200), in isoperibolic mode at 25 °C, using benzoic acid as a calibration standard.

The mass and energy yields of RDF chars (on a dry basis) were calculated based on Eqs. (1) and (2), respectively:

$$Mass\ yield\ (\%) = \frac{m_{char}}{m_{RDF}} \times 100 \quad (1)$$

$$Energy\ yield\ (\%) = Mass\ yield \times \frac{HHV_{char}}{HHV_{RDF}} \times 100 \quad (2)$$

where m_{char} and HHV_{char} are the mass (kg) and high heating value of RDF char (MJ/kg); m_{RDF} and HHV_{RDF} are the mass and high heating value of raw RDF.

Mineral composition of ash from RDF and RDF char samples was determined through X-Ray fluorescence (Niton XL 3T Gold++). Chlorine content was determined through an adaptation of ASTM D4208-02, using a bomb calorimeter (IKA C200) with Na_2CO_3 absorbing solution used during the combustion step and a chloride selective electrode (Hanna HI 4007) connected to a potentiometer (Hanna HI 98185).

2.4. Refuse derived fuel char leaching tests

Upgrading of the RDF chars by removal of water-soluble species was evaluated by two leaching tests: extraction with distilled water at room temperature and Soxhlet extraction also with distilled water. For the room temperature leaching test, an adaptation of EN 12457-2: 2002 was used. Briefly, the RDF char samples were mixed with distilled water in closed glass flasks, at an L/S ratio of 10 L/kg and constant temperature of 20 ± 2 °C. The flasks were shaken at 10 rpm (Heidolph Reax Top), for a period of 24 ± 0.5 h. For the Soxhlet extraction, the same L/S ratio was used as well as the same contact time. After both extraction procedures, the RDF char samples were filtered and oven dried (Memmert) at 105 ± 2 °C for 12 h. Chlorine content, HHV and ash content were measured in the decontaminated chars as described in Section 2.3.

2.5. Characterization of gaseous products

Torrefaction and carbonization gas products were analyzed by GC-TCD (Thermo Trace GC Ultra) for quantification of oxygen, carbon dioxide, carbon monoxide, hydrogen and methane. Total volatile organic compounds (VOCs) were determined using a total hydrocarbon analyzer (Signal, Model 3010), based on flame ionization detection and using propane as a calibration standard. The yield of the gaseous products was determined by difference between 100% and the sum of char mass yield and liquid fraction mass yield.

2.6. Characterization of liquid products

Liquid fraction mass yield was obtained by applying Eq. (1) and using the mass of collected condensate ($m_{condensates}$) instead of the mass of char.

The water content in the condensed phase was analyzed according to ASTM D95, using *o*-xylene and a Dean-Stark apparatus. Chemical oxygen demand (COD) was determined after open vessel digestion using the potassium dichromate methodology, as described in method 5220B from Standard Methods for the Examination of Water and Wastewater. Density was determined gravimetrically and the pH was measured with a pH meter (Crimson MicropH 2001).

Characterization of the organic fraction present in the condensed phase was performed by solvent extraction followed by GC–MS. The condensate samples (5 mL) were acidified until pH = 2 (H_2SO_4, 97%), to ensure protonation of weak acid species and extracted three times

with chloroform (2 mL each extraction). The combined extracts were dried with anhydrous sodium sulphate, filtered and derivatized with BSA (N,O-Bis(trimethylsilyl)acetamide), to convert the carboxylic functional groups into their trimethylsilyl derivatives. The chromatographic analysis of the extracts was performed using a GC–MS analyzer (Focus GC, Polaris Q – Thermo) equipped with a DB-5 capillary column (30 m length, 0.25 mm inner diameter and 0.25 μm film thickness). The extracts were injected in split mode, at 250 °C and the GC temperature was programmed as follows: initial temperature of 35 °C, held for 5 min, increased to 260 °C at a rate of 5 °C/min, and held for 1 min. The transfer line and ion source temperatures were 260 °C and 200 °C, respectively. The organic compounds present in the chloroform extracts were identified by comparing their mass spectra with those in NIST and WILEY databases and with the retention time and mass spectra of corresponding standards.

3. Results and discussion

3.1. Characterization of raw material and produced chars

The thermochemical upgrading process converted the raw RDF sample to RDF chars with a darker color and a more homogeneous appearance. In the char produced at 300 °C, it was still possible to detect particle color gradients corresponding to different materials, whereas the char produced at 400 °C had a uniform black color (Fig. S1, Supplementary data).

The tenacity of the RDF was reduced by thermal processing, since the produced chars were significantly more brittle than the original RDF, an advantageous characteristic for size reduction operations. According to observations by Verhoeff et al. (2011), raw RDF is difficult to mill, whereas after torrefaction, the produced char is easily milled at room temperature.

The main product of torrefaction or carbonization of the raw RDF was the solid char (62.9 and 82.0 wt%), but variable amounts of liquid and gas products were also formed during these processes, in proportions that were dependent on the process temperature (in Fig. 2). As expected, raising the temperature from 300 °C to 400 °C increased liquid and gas yields from 12.1 to 17.0 wt% and from 5.9 to 20.1 wt%, respectively. The reduction of the RDF mass during thermal treatment is due to the vaporization of water and volatile components and to the thermochemical decomposition of RDF to yield low to medium molecular weight products, a process that occurs at a larger extent for higher temperatures.

The chemical compositions of the raw RDF and of the corresponding chars showed noticeable differences, as detailed in Table 1. While the original RDF sample had a moisture content of around 10 wt%, the RDF chars presented residual moisture contents (below 1.5 wt%) which is an advantage regarding storage and transportation, since high moisture contents are related to low calorific values and microbial degradation (Samad et al., 2017).

Significant devolatilization was observed at both temperatures, leading to a decrease in volatile matter of the chars formed at 300 °C and 400 °C (56.3 and 47.6 wt%, respectively) when compared to the volatile matter of raw RDF (74.9 wt%). The RDF mass loss observed at

Table 1
Chemical properties of raw RDF and produced RDF chars, expressed as average values (± standard deviation).

Parameter	Unit	RDF	RDF char (300 °C, 30 min)	RDF char (400 °C, 30 min)
Proximate analysis				
Moisture	wt.%, ar[a]	10.5 ± 0.4	1.3 ± 0.1	0.4 ± 0.0
Volatile matter	wt.%, db[b]	74.9 ± 1.4	56.3 ± 0.5	47.6 ± 1.3
Ash		16.9 ± 1.4	22.8 ± 0.3	28.8 ± 0.4
Fixed carbon		8.2 ± 0.5	20.9 ± 0.4	23.6 ± 1.6
Ultimate analysis				
C	wt.%, daf[c]	41.1 ± 1.4	61.0 ± 0.1	80.2 ± 0.1
N		2.5 ± 0.0	1.3 ± 0.0	1.9 ± 0.1
H		5.6 ± 0.3	6.2 ± 0.0	8.4 ± 0.1
S		0.4 ± 0.0	0.3 ± 0.0	0.3 ± 0.0
O		50.4 ± 1.1	31.2 ± 0.1	9.2 ± 0.2
Ash mineral composition				
Ca	wt.%, db	50.6 ± 2.1	34.1 ± 2.0	36.8 ± 2.4
Fe		3.1 ± 0.7	13.9 ± 1.6	12.2 ± 0.8
Ti		5.5 ± 0.1	8.6 ± 1.7	9.0 ± 1.4
Cu		0.4 ± 0.0	6.3 ± 0.3	4.9 ± 0.2
Zn		2.9 ± 0.2	6.8 ± 0.1	7.0 ± 0.0
K		6.0 ± 0.6	4.0 ± 0.1	3.8 ± 0.3
Si		21.6 ± 3.2	16.3 ± 1.2	16.1 ± 1.9
Al		7.9 ± 0.1	4.4 ± 0.6	4.7 ± 0.9
Mg		–	–	–
P		–	1.3 ± 0.0	0.5 ± 0.1
Others		2.0	4.3	5.0
Cl	wt.%, db	0.7 ± 0.1	1.8 ± 0.0	1.9 ± 0.1
HHV	MJ/kg, db	16.4 ± 0.1	19.9 ± 0.1	23.5 ± 0.0
Energy yield	%, db	–	98.3	85.6

[a] ar – as received basis.
[b] db – dry basis.
[c] daf – dry ash free basis.

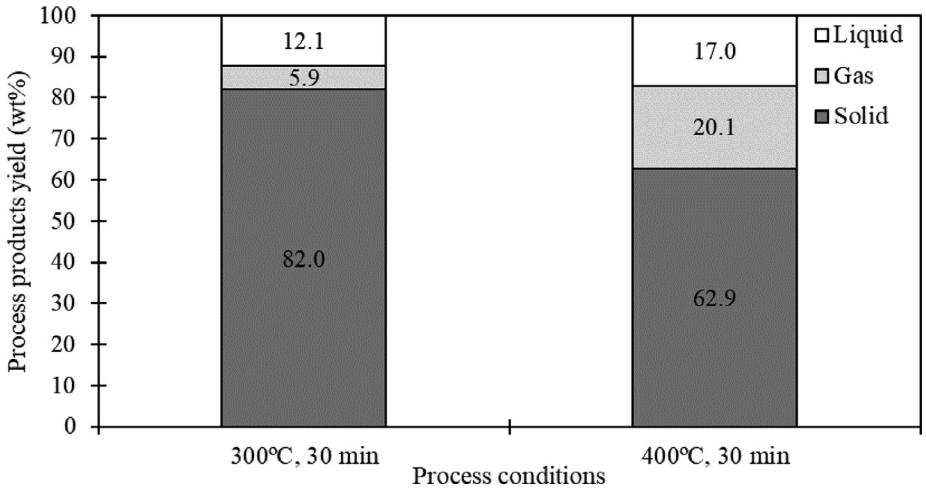

Fig. 2. Solid, liquid and gaseous products distribution (wt.%) obtained with RDF torrefaction (300 °C) and carbonization (400 °C).

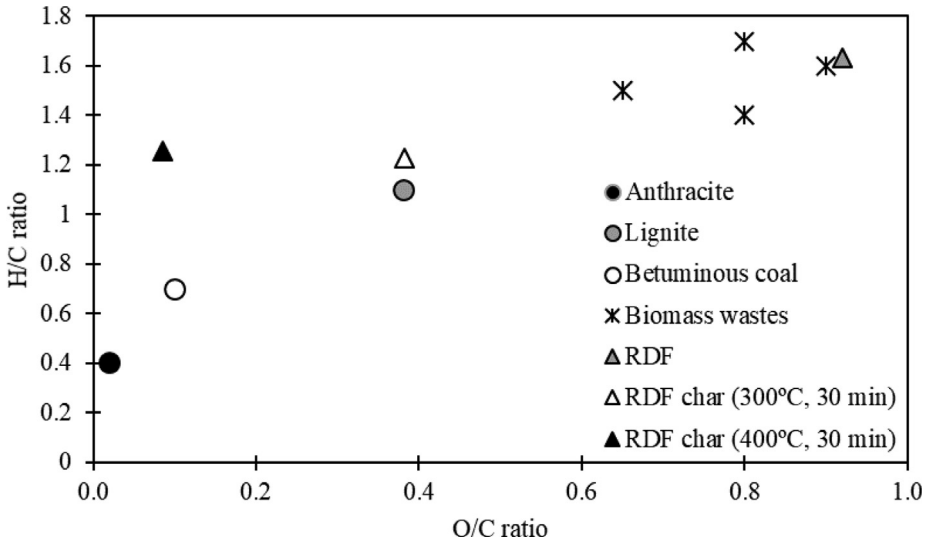

Fig. 3. Van Krevelen diagram for the RDF and RDF chars produced at 300 °C and 400 °C. Fossil fuels and biomass wastes are shown for comparison (van der Stelt et al., 2011).

300 °C can be mainly attributed to the decomposition of lignocellulosic materials, since hemicellulose, cellulose and lignin, are susceptible to thermal decomposition in the temperature range of 225–500 °C (Prins et al., 2006a; Qi et al., 2018). At 400 °C, both fractions are susceptible to thermal decomposition, as most polymeric materials decompose at higher temperatures, in the range of 350–550 °C, due to the high stability of the C—C bonds, that support their polymeric structures (Haykiri-Acma et al., 2017; López et al., 2011; Park et al., 2012).

As moisture and volatile matter are eliminated from the RDF, the non-volatile components (fixed carbon and ash) are concentrated in the RDF char. Ash content reached values of 22.8 and 28.8 wt%, for the chars produced at 300 °C and 400 °C. These values represent an increment of 5.8 and 11.9%, respectively, relatively to the ash content of the raw RDF. On the other hand, fixed carbon also increased from 8.2 wt% for raw RDF to 20.9 wt% and 23.6 wt% for the RDF chars produced at 300 °C and 400 °C, respectively. This outcome is a common feature of these thermochemical processes and has been described by other authors using RDF and MSW and biomass (Białowiec et al., 2017; Recari et al., 2017; Samad et al., 2017). As these two parameters (ash and fixed carbon) have opposite effects on the fuel heating value, the thermochemical conditions should be chosen in order to maximize this fuel property.

High ash chars have limited application as fuels in combustion or gasification because there are several related operational issues such as excessive ash deposition or slagging and fouling phenomena (Akdag et al., 2016). The co-combustion of high-ash chars with less problematic fuels, such as biomass or coal can still enable their energetic valorization with lower operational drawbacks (Casado et al., 2016). In alternative to fuel applications, RDF chars may be explored for their material valorization as activated carbon precursors (Gopu et al., 2018; Hajizadeh and Williams, 2013). The quality of solid fuels is not only influenced by ash content but also by ash composition, therefore that was a parameter determined for raw RDF and the RDF chars (Table 1). Ash composition determines its melting point thus affecting the fuel tendency to form solid deposits inside boilers or gasifiers. The main components detected in the raw RDF and in the RDF char ash were calcium and silica (> 15 wt%). Aluminum, potassium, zinc, titanium, iron and copper were present at concentrations lower than 15 wt% and phosphorus was only detected in the RDF chars. A group of minor components with concentrations lower than 1 wt% was not presented individually but as a sum of other mineral components (Table 1). The torrefaction and carbonization processes caused an increase in the concentration of all mineral components relatively to the raw RDF, except for calcium, silica, potassium and aluminum. Also, the concentrations of iron, copper, potassium silica and phosphorus did not increase with the severity of the thermochemical process, when the temperature was increase from 300 °C to 400 °C, regardless of the decrease in char yield. This indicates that another process besides the concentration effect of RDF mass loss is influencing the concentration of the non-volatile inorganic fraction. A possible explanation is the dissolution or entrainment of the more abundant mineral components by the process condensates, that are mainly composed of water. This phenomenon is analogous to the dissolution of inorganic components during hydrothermal carbonization (Reza et al., 2013) and may occur especially during the cooling phase of condensates and chars. A similar process explains the deposition of tar components in the carbonaceous structure of the char, during torrefaction or carbonization of biomass fuels (Kuzmina et al., 2016).

Bond breaking during torrefaction or carbonization favors the elimination of more electronegative elements such as oxygen or nitrogen relatively to carbon or hydrogen (Vollhardt and Schore, 2007), a tendency that will influence the elemental composition of the formed chars. Ultimate analysis showed that carbon content increased from 41.1 wt% to 61.0 wt% and 80.2 wt%, for the RDF chars produced at 300 °C and 400 °C, respectively. Hydrogen content also increased with process temperature although in a less pronounced way, reaching the highest value at 400 °C (8.4 wt%). On the other hand, oxygen content that was relatively high for the raw RDF (50.4 wt%) due to the presence of the lignocellulosic materials, decreased to 31.2 and 9.2 wt% for the RDF chars produced at 300 °C and 400 °C, respectively. The release of volatile oxygenated compounds during decomposition of hemicellulose, cellulose and lignin from the RDF biomass component is the possible mechanism by which carbon is concentrated in the RDF chars (Yue et al., 2017). Nitrogen and sulphur in RDF are also partially eliminated during torrefaction or carbonization because their polar covalent bonds with carbon atoms are easier to break than the non-polar C—C bonds that are relatively stable up to 400 °C. As a consequence, the RDF chars presented lower concentrations of nitrogen and sulphur than the raw RDF, a positive characteristic regarding harmful NOx and SOx emissions during combustion.

The relation between H/C ratio and O/C ratio for the raw RDF and resulting RDF chars is compared in Fig. 3 with similar data reported in the literature for different biofuels and fossil fuels showed for comparison. While raw RDF had a composition comparable to biomass wastes, the RDF chars presented much lower O/C ratios, similar to lignite (RDF char produced at 300 °C) or to bituminous coal (RDF char

produced at 400 °C). The H/C ratio of both chars is lower than the raw RDF, but higher than bituminous coal or lignite reflecting a lower degree of aromatization of the RDF chars when compared with these fossil fuels. The elemental composition differences observed between raw RDF and the RDF chars clearly depicts a fuel upgrading effect brought by torrefaction and carbonization, regarding water removal and oxygen elimination in the form of oxygenated volatile compounds through decarboxylation, decarbonylation and dehydration reactions (Yue et al., 2017) occurring in both processes but more extensively in the carbonization range.

Oxygen reduction and carbon increase are also the primary reasons for the increase in HHV of the RDF chars (Table 1). The char obtained at 300 °C had a HHV of 19.9 MJ/kg while the char produced at 400 °C had a HHV of 23.5 MJ/kg, values that are respectively, 21 and 43% higher than the HHV of the raw RDF (16.4 MJ/kg).

Energy yield was 98.3% and 85.6%, for the processes at 300 °C and 400 °C, respectively, although the RDF char obtained at 400 °C had a higher HHV than the one obtained at 300 °C. At 400 °C a higher fraction of the RDF carbon was lost to the vapor phase, reducing mass yield to an extent that overcomes the influence of the RDF char heating value on the energy yield. According to van der Stelt et al. (2011), although there is a 30 wt% mass loss during torrefaction, the torrefied product can retain up to 90% of the energy content, which is in accordance with the mass and energy yields obtained in the present work. This increase in energy density after both thermochemical treatments is of high relevance for the adaptation of these processes to an industrial scale because of the consequences at the levels of product quality, transportation and logistics (Recari et al., 2017; van der Stelt et al., 2011).

Chlorine content in the produced RDF chars was higher when compared to the raw RDF, and increased with the treatment temperature, reaching values of 1.8 and 1.9 wt%, at 300 °C and 400 °C, respectively (Table 1). According to Hwang et al. (2007) these chlorine values are high enough to cause problems during combustion, with the potential to damage several components of the thermal conversion system due to high temperature corrosion. Contrary to the results obtained in this work, several authors report a decrease in chlorine content for RDF or MSW after torrefaction or carbonization (Edo et al., 2017; Recari et al., 2017; Yuan et al., 2015). The chlorine content, due to its volatility, is reduced after the carbonization process, transitioning to the condensable and non-condensable gas phase (Edo et al., 2017). The increase in chlorine content may be associated with chlorine recondensation on the RDF char surface, or chlorine adsorbed onto the organic and mineral phases of the RDF char (Vassilev et al., 1999). Additionally, chlorine from the plastic component (PVC) of RDF is almost completely released under 400 °C, but there is also potential for the formation of inorganic salts such as potassium or calcium chloride, which have boiling points significantly above 400 °C (Hwang et al., 2006; Vassilev et al., 1999). This behavior can be expected for the torrefaction or carbonization of chlorine-containing polymers in industrial units that are not usually equipped with gas purging systems by injection of an inert gas, because the continuous injection of a purging gas during the torrefaction or carbonization process increases costs and energy requirements of the processes by introducing another material input and potentially lowering the operating temperature (Sarvaramini and Larachi, 2014).

To evaluate the potential of water leaching in the upgrading of the RDF chars by chorine dissolution, the RDF char was subject to leaching experiments, with water at room temperature and with water close to its boiling point, using a Soxhlet apparatus (Fig. 4). These experiments aimed to evaluate whether chlorine was chemically bonded to the char structure or simply adsorbed on its surface or pores and therefore accessible to water solvation.

Both water leaching tests caused a reduction of chlorine content in the RDF chars, indicating that this element is present in the form water-soluble chlorine compounds, that were formed during the torrefaction and carbonization experiments. The decrease was more accentuated in the RDF char produced at 400 °C with Soxhlet extraction, reaching a chlorine concentration of 0.544 wt%, which is below the chlorine concentration of the raw RDF. Although carbonization at 400 °C is expected to lead to a higher dichlorination degree than torrefaction at 300 °C, the chlorine content of the char obtained at 300 °C was lower. This observation suggests that the char produced at 400 °C may have a more organized structure with a higher porosity that is more favorable to chlorine adsorption. Other mineral components were also removed by the leaching processes since the ash content in the RDF chars decreased around 1% for both chars after water leaching at room temperature and around 3% after Soxhlet extraction, which is beneficial to the RDF chars fuel properties. In particular, HHV of both chars was increased by the washing treatments, reaching values of 22.5 and 26.7 MJ/kg for the chars produced at 300 and 400 °C, respectively, after the Soxhlet extraction with water. Nevertheless, this final treatment with hot water must be optimized to minimize water use, by recycling the water through an ion exchange unit, and the associated energy consumption must be considered in the process energetic balances.

3.2. Characterization of gaseous products

The release of gaseous products during torrefaction or carbonization occurs either by evaporation or thermal decomposition of the raw materials. The amount of torrefaction emissions produced depends on the composition of raw material, heating rate, temperature and residence time (Stelte, 2012). The concentrations of the main gas products from torrefaction and carbonization of RDF are presented in Fig. 5. Excluding water, the major gas products from RDF torrefaction and carbonization were carbon dioxide and carbon monoxide, which is expected from the thermal decomposition in an oxygen deficient atmosphere. Carbon dioxide, carbon monoxide and water are formed by decarboxylation, decarbonylation and dehydration reactions, that occur during the thermal decomposition of lignocellulosic materials (White and Dietenberger, 2001). There were also traces of hydrogen, with higher concentrations at 400 °C, while methane could only be detected at 400 °C. According to Wahid et al. (2017), at higher temperatures, methane may be formed through methanation (reaction of carbon monoxide with hydrogen to yield methane and water).

Both process conditions yielded a concentration of volatile organic compounds (VOCs) of 1280 ppm (expressed in total carbon). The composition of the gas products obtained in this work are in line with other studies using different raw materials, such as willow, starch, straw and larch (Prins et al., 2006b) or RDF and Stabilat (Stelte, 2012).

3.3. Characterization of liquid products

Condensates from the torrefaction and carbonization of RDF included liquid formed and collected in two condensation chambers (1st and 2nd collection points), as previously described (Section 2.2). Liquid fractions from the torrefaction process presented a lighter color than the ones produced at 400 °C, a sign of the more extensive decomposition occurring at the higher temperature. Moreover, condensates collected in the 1st collection point had a darker color and appeared to have particulate matter in suspension, probably corresponding to heavy non-polar products. The condensates collected in the 2nd collection point, had a lighter color and presented an oily upper layer, composed of water-insoluble liquid products (Fig. S2, Supplementary data).

As shown in Fig. 1, condensate yield was 12.1 wt% at 300 °C (635 mL) and 17.0 wt% at 400 °C (992 mL), reflecting the influence of temperature increase on the thermochemical decomposition of the raw RDF. At both collection points, the condensates had water contents of 95% and 90% for 300 °C and 400 °C, respectively (Table 2). A lower water content (45–56%) was found in the condensates produced during the torrefaction of bamboo between 250 and 350 °C (Chen et al., 2015). Chemical oxygen demand (COD) of the condensates recovered at the 2nd collection point, was higher than the COD of the condensates

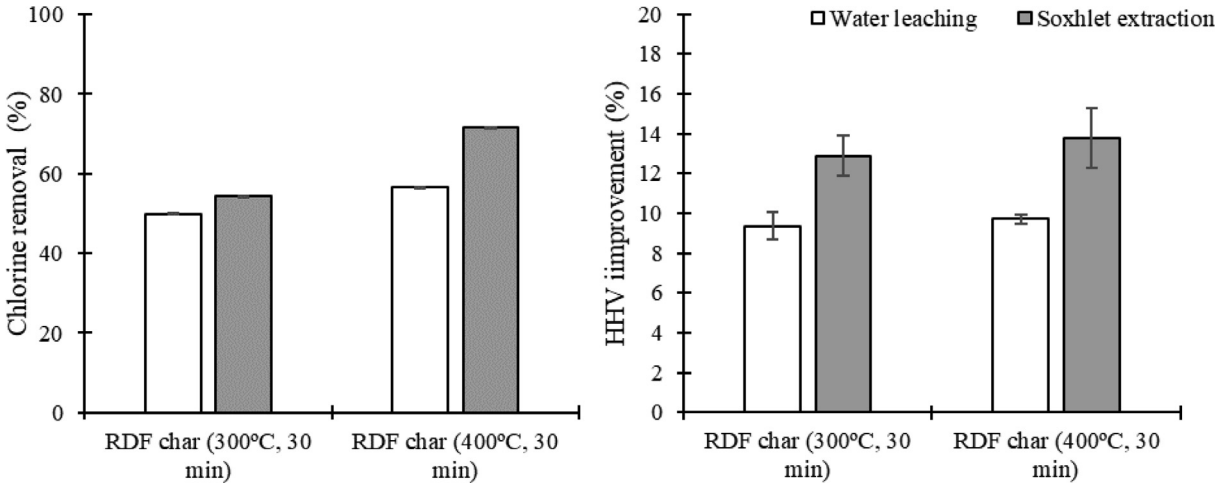

Fig. 4. Chlorine removal efficiency (%) and high heating value (HHV) improvement (%) for the RDF chars produced at 300 °C and 400 °C, after water leaching and Soxhlet extraction.

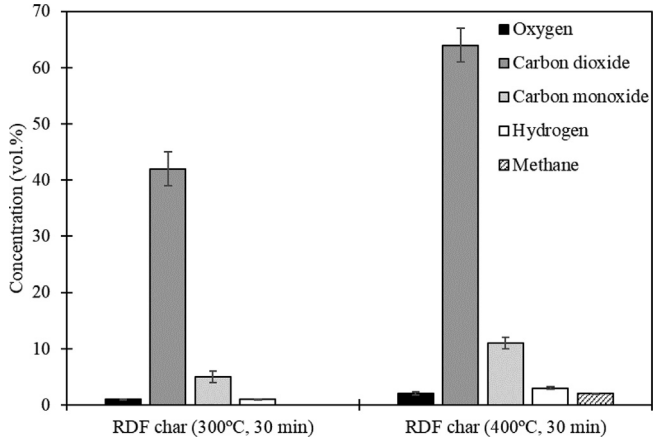

Fig. 5. Composition of gas products for RDF torrefaction (300 °C) and carbonization (400 °C).

recovered from the 1st collection point, suggesting that volatile organic components only recovered in the second condensation chamber contribute to this higher value. COD also increased with the process temperature, reaching a value of 69.3 g O_2/L, for the condensate collected in the 2nd collection point, after carbonization at 400 °C. The obtained values indicate that these liquid phases have very significant amounts of suspended and dissolved solids that must be removed before discharging this effluent. Nevertheless, these COD values are inferior to those measured by Fagërnas et al. (2015) for condensates from the torrefaction of spruce and bamboo, at temperatures of 240–300 °C. The higher water contents and the lower COD values of the condensates obtained in this work relatively to those reported (Chen et al., 2015; Fagërnas et al., 2015) concerning torrefaction of lignocellulosic materials, may be related with RDF composition, since the polymeric fraction is less susceptible to thermal degradation than the lignocellulosic biomass but also with the possible adsorption of tar components on the char surfaces. This process is avoided in torrefaction systems with injection of a purging inert gas, but has the advantage of promoting a higher retention of carbonaceous species from the condensates in the char products therefore increasing their yield (Kuzmina et al., 2016).

The pH of all condensate samples was acidic, reflecting the presence of organic acids, which are typical products of lignocellulosic biomass degradation (Chen et al., 2015; Tumuluru et al., 2011).

The identification of the major organic compounds found in the chloroform extracts of the condensates and their relative chromatographic peak areas are presented in Table 3. At 400 °C, in both collection points, it was possible to identify a larger number of compounds, as well as heavier compounds, evidencing a higher degree of tar formation at this temperature. Increasing process temperature yielded a higher number of phenols and carbonyl derivatives, which could be the result of a more extensive decomposition of lignin from the RDF biomass component (Chua et al.,2017). Also, more aromatic hydrocarbon molecules were identified at 400 °C, including two polycyclic aromatic hydrocarbons (naphthalene and phenanthrene), which is expected because higher temperatures favor condensation of aromatic compounds to form polycyclic structures (Richter and Howard, 2000). Furans, alcohols and monocyclic aromatic hydrocarbons were consistently more abundant in the 2nd collection point as a consequence of the relatively high volatility of those components, relatively to condensed aromatic hydrocarbons or phenols.

A higher presence of phenolic compounds at 400 °C was also detected. Furfural and 5-methylfurfural presented the largest peak areas within the furan group, similarly to biomass torrefaction tars in which these compounds are abundant as the result of direct ring-opening and

Table 2
Characterization of RDF torrefaction and carbonization liquid products. Results presented as average values (± standard deviation).

Parameters	Unit	Process temperature			
		300 °C		400 °C	
		1st collection point	2nd collection point	1st collection point	2nd collection point
Density	g/cm^3	0.99 ± 0.02	0.98 ± 0.03	1.00 ± 0.03	1.00 ± 0.02
Water content	wt.%	95 ± 0	95 ± 0	90 ± 0	90 ± 0
COD	g O_2/L	13.5 ± 2.7	36.5 ± 3.6	39.2 ± 0.0	69.3 ± 6.9
pH		3 ± 0	4 ± 0	3 ± 0	2 ± 0

Table 3
GC–MS relative peak areas of the main organic compounds found in the chloroform extracts from the condensates obtained in RDF torrefaction (300 °C) and carbonization (400 °C) experiments.

Compounds	Molecular formula	Relative peak area (%)			
		300 °C		400 °C	
		1st collection point	2nd collection point	1st collection point	2nd collection point
Acids					
Acetic acid	$C_2H_4O_2$	6.87	0.55	1.17	2.16
Oxalic acid	$C_2H_4O_4$	–	–	–	11.97
Propionic acid	$C_3H_6O_2$	2.59	0.58	2.52	1.48
Butyric acid	$C_4H_8O_2$	2.14	–	0.62	–
2-Methyl-2-furoic acid	$C_6H_6O_3$	0.76	–	0.74	–
Benzoic acid	$C_7H_6O_2$	21.40	0.35	21.80	1.06
Aldehydes					
4,4-Dimethyl-2-pentynal	$C_7H_{10}O$	–	1.75	0.87	0.37
Ketones					
2-Ethylcyclopentanone	$C_7H_{12}O$	–	–	4.02	0.48
Dihydroxyacetophenone	$C_8H_8O_3$	0.73	–	0.77	0.40
Guaiacylacetone	$C_{10}H_{12}O_3$	–	–	1.22	0.16
3-Hidroxy-2-methyl-4H-pyran-4-one	$C_6H_6O_3$	1.06	1.33	2.68	1.75
Alcohols					
Butanol	$C_4H_{10}O$	0.95	3.28	1.29	1.81
2-Chloroethanol	ClC_2H_5O	1.93	2.59	1.33	1.57
Octanol	$C_8H_{18}O$	–	1.36	–	1.38
Esters					
Hydroxyethylbenzoate	$C_9H_{10}O_3$	–	–	3.04	–
Ethers					
2,4,6-Trimethyl-(2α,4α,6α)-1,3-dioxane	$C_6H_6O_3$	–	–	0.53	< 0.10
Furans					
Furfural	$C_5H_4O_2$	17.4	50.31	13.82	7.22
2,4-Dimethyl-furan	C_6H_8O	0.22	–	0.59	–
Acetylfuran	$C_6H_6O_2$	0.97	0.85	1.69	0.76
5-Methylfurfural	$C_6H_6O_2$	7.40	10.30	8.18	4.28
Aromatic hydrocarbons					
1,1-Biphenyl	$(C_6H_5)_2$	0.64	0.30	–	0.56
Benzonitrile	C_6H_5CN	–	0.94	0.67	0.42
Ethylbenzene	C_8H_{10}	–	–	–	0.28
Xylene	C_8H_{10}	–	–	–	0.31
Styrene	C_8H_8	–	–	–	1.65
2-Propenylbenzene	C_9H_{10}	–	–	–	0.47
1-Ethyl-2-methylbenzene	C_9H_{12}	–	–	–	0.35
Cumene	C_9H_{12}	–	0.49	–	0.16
Naphtalene	$C_{10}H_8$	–	–	–	0.32
Phenatrene	$C_{14}H_{10}$	–	–	–	0.46
Phenols					
Phenol	C_6H_6O	4.27	1.98	9.01	2.22
4-Methoxyphenol	$C_7H_8O_2$	–	–	1.59	–
2-Methoxy-4-methylphenol	$C_8H_{10}O_2$	–	–	0.60	–
2,6-Dimethoxyphenol	$C_8H_{10}O_3$	0.42	–	1.15	–
3,4-Dimethoxyphenol	$C_8H_{10}O_3$	–	–	0.84	–
Hydroquinone	$C_6H_6O_2$	0.88	–	0.50	–
Terpenes					
3-carene	$C_{10}H_{16}$	0.26	0.47	–	0.51
Total identified peaks (% peak area)		70.89	77.43	77.22	44.08

rearrangement reactions of cellulose molecules (Shen and Gu, 2009). The abundance of oxygenated compounds in the condensates from RDF torrefaction or carbonization is an evidence of the deoxygenation of the original raw material, justifying the low oxygen content of the chars formed at both process temperatures (Chen et al., 2018a).

The volume and complex composition of the condensates collected during these processes represents one of the main issues that must be addressed when scaling up the torrefaction process. The recirculation of torrefaction condensates through the raw materials prior to the thermal conversion process to retain organic molecules (Chen et al., 2017), the separation of different organic compounds with added value (acetic acid, furfural, phenol) (Fagërnas et al., 2015) or the use of these tars as additives in biomass pelletizing processes (Stelte, 2012), are some of the processes proposed in literature to minimize the environmental impact of these condensates and recover some of their organic content.

4. Conclusions

Torrefaction (300 °C) and carbonization (400 °C), converted RDF to chars with higher carbon content and calorific value, thus upgrading the composition and properties of this waste derived fuel. Ash and chlorine concentrations increased with process temperature, but could be reduced by subsequent washing with hot water, yielding chars with even higher calorific values. Gaseous emissions were mainly composed

of carbon dioxide and carbon monoxide, with smaller amounts of methane and hydrogen. Liquid emissions presented very high COD values and were mostly composed by water and organic oxygenated compounds such as acids, furans and phenols.

Acknowledgements

This work was supported by the CITRI, S.A. project I&DT n° 24878; and by the Portuguese Foundation for Science and Technology (grant no. SFRH/BD/111956/2015), co-financed by the Operational Program Human Potential and the European Social Fund-European Union.

Appendix A. Supplementary material

Supplementary data to this article can be found online at https://doi.org/10.1016/j.biortech.2019.121325.

References

Akdag, A.S., Atimtay, A., Sanin, F.D., 2016. Comparison of fuel value and combustion characteristics of two different RDF samples. Waste Manag. 47, 217–224. https://doi.org/10.1016/j.wasman.2015.08.037.

Anthraper, D., McLaren, J., Baroutian, S., Munir, M.T., Young, B.R., 2018. Hydrothermal deconstruction of municipal solid waste for solid reduction and value production. J. Clean. Prod. 201, 812–819. https://doi.org/10.1016/j.jclepro.2018.08.116.

Astrup, T.F., Tonini, D., Turconi, R., Boldrin, A., 2014. Life cycle assessment of thermal Waste-to-Energy technologies: review and recommendations. Waste Manag. 37, 104–115. https://doi.org/10.1016/j.wasman.2014.06.011.

Beyene, H.D., Werkneh, A.A., Ambaye, T.G., 2018. Current updates on waste to energy (WtE) technologies: a review. Renew. Energy Focus 24, 1–11. https://doi.org/10.1016/j.ref.2017.11.001.

Białowiec, A., Pulka, J., Stępień, P., Manczarski, P., Gołaszewski, J., 2017. The RDF/SRF torrefaction: an effect of temperature on characterization of the product – Carbonized Refuse Derived Fuel. Waste Manag. 70, 91–100. https://doi.org/10.1016/j.wasman.2017.09.020.

Casado, R.R., Rivera, J.A., García, Borjabad, E., Cuadrado, R.E., Llorente, M.F., Sevillano, R.B., Delgado, A.P., 2016. Classification and characterisation of SRF produced from different flows of processed MSW in the Navarra region and its co-combustion performance with olive tree pruning residues. Waste Manag. 47, 206–216. https://doi.org/10.1016/j.wasman.2015.05.018.

Chen, D., Cen, K., Cao, X., Li, Y., Zhang, Y., Ma, H., 2018a. Restudy on torrefaction of corn stalk from the point of view of deoxygenation and decarbonization. J. Anal. Appl. Pyrolysis 135, 1–9. https://doi.org/10.1016/j.jaap.2018.09.015.

Chen, D., Gao, A., Ma, Z., Fei, D., Chang, Y., Shen, C., 2018b. In-depth study of rice husk torrefaction: characterization of solid, liquid and gaseous products, oxygen migration and energy yield. Bioresour. Technol. 253, 148–153. https://doi.org/10.1016/j.biortech.2018.01.009.

Chen, D., Mei, J., Li, H., Li, Y., Lu, M., Ma, T., Ma, Z., 2017. Combined pretreatment with torrefaction and washing using torrefaction liquid products to yield upgraded biomass and pyrolysis products. Bioresour. Technol. 228, 62–68. https://doi.org/10.1016/j.biortech.2016.12.088.

Chen, W.-H., Liu, S.-H., Juang, T.-T., Tsai, C.-M., Zhuang, Y.-Q., 2015. Characterization of solid and liquid products from bamboo torrefaction. Appl. Energy 160, 829–835. https://doi.org/10.1016/j.apenergy.2015.03.022.

Chua, Y.W., Yu, Y., Wu, H., 2017. Thermal decomposition of pyrolytic lignin under inert conditions at low temperatures. Fuel 200, 70–75. https://doi.org/10.1016/j.fuel.2017.03.035.

Chyang, C.S., Han, Y.L., Wu, L.W., Wan, H.P., Lee, H.T., Chang, Y.H., 2010. An investigation on pollutant emissions from co-firing of RDF and coal. Waste Manag. 30, 1334–1340. https://doi.org/10.1016/j.wasman.2009.11.018.

Dalai, A.K., Batta, N., Eswaramoorthi, I., Schoenau, G.J., 2009. Gasification of refuse derived fuel in a fixed bed reactor for syngas production. Waste Manag. 29, 252–258. https://doi.org/10.1016/j.wasman.2008.02.009.

Edo, M., Skoglund, N., Gao, Q., Persson, P., Jansson, S., 2017. Fate of metals and emissions of organic pollutants from torrefaction of waste wood, MSW, and RDF. Waste Manag. 68, 646–652. https://doi.org/10.1016/j.wasman.2017.06.017.

Fagërnas, L., Kuoppala, E., Arpiainen, V., 2015. Composition, utilization and economic assessment of torrefaction condensates. Energy&Fuels 29, 3134–3142. https://doi.org/10.1021/acs.energyfuels.5b00004.

Fellner, J., Aschenbrenner, P., Cencic, O., Rechberger, H., 2011. Determination of the biogenic and fossil organic matter content of refuse-derived fuels based on elementary analyses. Fuel 90, 3164–3171. https://doi.org/10.1016/j.fuel.2011.06.043.

Gopu, C., Gao, L., Volpe, M., Fiori, L., Goldfarb, J.L., 2018. Valorizing municipal solid waste: waste to energy and activated carbons for water treatment via pyrolysis. J. Anal. Appl. Pyrolysis 133, 48–58. https://doi.org/10.1016/j.jaap.2018.05.002.

Hajizadeh, Y., Williams, P.T., 2013. Activated carbon production from RDF and its use for dioxin removal from flue gas of waste incinerators. Int. J. Environ. Health Eng. 1, 1–10. https://doi.org/10.4103/2277-9183.110131.

Haykiri-Acma, H., Kurt, G., Yaman, S., 2017. Properties of biochars obtained from RDF by carbonization: influences of devolatilization severity. Waste Biomass Valorization 8, 539–547. https://doi.org/10.1007/s12649-016-9610-5.

Hwang, I.H., Matsuto, T., Tanaka, N., 2006. Water-soluble characteristics of chlorine in char derived from municipal solid wastes. Waste Manag. 26, 571–579. https://doi.org/10.1016/j.wasman.2005.04.012.

Hwang, I.H., Matsuto, T., Tanaka, N., Sasaki, Y., Tanaami, K., 2007. Characterization of char derived from various types of solid wastes from the standpoint of fuel recovery and pretreatment before landfilling. Waste Manag. 27, 1155–1166. https://doi.org/10.1016/j.wasman.2006.05.013.

Kuzmina, J.S., Director, L.B., Shevchenko, A.L., Zaichenko, V.M., 2016. Energy efficiency analysis of reactor for torrefaction of biomass with direct heating. J. Phys. Conf. Ser. 774. https://doi.org/10.1088/1742-6596/774/1/012138.

López, A., De Marco, I., Caballero, B.M., Laresgoiti, M.F., Adrados, A., 2011. Influence of time and temperature on pyrolysis of plastic wastes in a semi-batch reactor. Chem. Eng. J. 173, 62–71. https://doi.org/10.1016/j.cej.2011.07.037.

Nasrullah, M., Vainikka, P., Hannula, J., Hurme, M., 2015. Elemental balance of SRF production process: solid recovered fuel produced from commercial and industrial waste. Fuel 145, 1–11. https://doi.org/10.1016/j.fuel.2014.12.071.

Nobre, C., Gonçalves, M., Vilarinho, C., 2019. A brief assessment on the application of torrefaction and carbonization for refuse derived fuel upgrading. Lect. Notes Electr. Eng. 505, 633–640. https://doi.org/10.1007/978-3-319-91334-6_86.

Park, S.S., Seo, D.K., Lee, S.H., Yu, T.U., Hwang, J., 2012. Study on pyrolysis characteristics of refuse plastic fuel using lab-scale tube furnace and thermogravimetric analysis reactor. J. Anal. Appl. Pyrolysis 97, 29–38. https://doi.org/10.1016/j.jaap.2012.06.009.

Prins, M.J., Ptasinski, K.J., Janssen, F.J.J.G., 2006a. Torrefaction of wood. Part 1. Weight loss kinetics. J. Anal. Appl. Pyrolysis 77, 28–34. https://doi.org/10.1016/j.jaap.2006.01.002.

Prins, M.J., Ptasinski, K.J., Janssen, F.J.J.G., 2006b. Torrefaction of wood. Part 2. Analysis of products. J. Anal. Appl. Pyrolysis 77, 35–40. https://doi.org/10.1016/j.jaap.2006.01.001.

Qi, J., Zhao, J., Xu, Y., Wang, Y., Han, K., 2018. Segmented heating carbonization of biomass: yields, property and estimation of heating value of chars. Energy 144, 301–311. https://doi.org/10.1016/j.energy.2017.12.036.

Rada, E.C., Andreottola, G., 2012. RDF/SRF: which perspective for its future in the EU. Waste Manag. 32, 1059–1060. https://doi.org/10.1016/j.wasman.2012.02.017.

Recari, J., Berrueco, C., Puy, N., Alier, S., Bartrolí, J., Farriol, X., 2017. Torrefaction of a solid recovered fuel (SRF) to improve the fuel properties for gasification processes. Appl. Energy 203, 177–188. https://doi.org/10.1016/j.apenergy.2017.06.014.

Reza, M.T., Lynam, J.G., Uddin, M.H., Coronella, C.J., 2013. Hydrothermal carbonization: fate of inorganics. Biomass Bioenergy 49, 86–94. https://doi.org/10.1016/j.biombioe.2012.12.004.

Richter, H., Howard, J.B., 2000. Formation of polyciclic aromatic hydrocarbons and their growth to soot – a review of chemical reaction pathways. Prog. Energy Combust. Sci. 26, 565–608. https://doi.org/10.1016/S0360-1285(00)00009-5.

Samad, N.A.F.A., Jamin, N.A., Saleh, S., 2017. Torrefaction of municipal solid waste in Malaysia. Energy Proc. 138, 313–318. https://doi.org/10.1016/j.egypro.2017.10.106.

Sarvaramini, A., Larachi, F., 2014. Integrated biomass torrefaction – chemical looping combustion as a method to recover torrefaction volatiles energy. Fuel 116, 158–167. https://doi.org/10.1016/j.fuel.2013.07.119.

Shen, D.K., Gu, S., 2009. The mechanism for thermal decomposition of cellulose and its main products. Bioresour. Technol. 100, 6496–6504. https://doi.org/10.1016/j.biortech.2009.06.095.

Silva, R.B., Fragoso, R., Sanches, C., Costa, M., Martins-Dias, S., 2014. Which chlorine ions are currently being quantified as total chlorine on solid alternative fuels? Fuel Process Technol. 128, 61–67. https://doi.org/10.1016/j.fuproc.2014.07.003.

Stelte, W., 2012. Torrefaction of unutilized biomass resources and characterization of torrefaction gases. Resultat Kontrakt (RK) Report – Danish Technological Institute.

Tumuluru, J.S., Sokhansanj, S., Hess, J.R., Wright, C.T., Boardman, R.D., 2011. A review on biomass torrefaction process and product properties for energy applications. Ind. Biotechnol. 7, 384–401. https://doi.org/10.1089/ind.2011.0014.

van der Stelt, M., Gerhauser, H., Kiel, J., Ptasinski, K., 2011. Biomass upgrading by torrefaction for the production of biofuels: a review. Biomass Bioenergy 35, 3748–3762. https://doi.org/10.1016/j.biombioe.2011.06.023.

Vassilev, S.V., Braekman-Danheux, C., Laurent, P., Thiemann, T., Fontana, A., 1999. Behaviour, capture and inertization of some trace elements during combustion of refuse-derived char from municipal solid waste. Fuel 78, 1131–1145. https://doi.org/10.1016/S0016-2361(99)00043-5.

Verhoeff, F., Adell i Arnuelos, A., Boersma, A.R., Pels, J.R., Lensselink, J., Kiel, J.H.A., Schukken, H., 2011. TorTech: torrefaction technology for the production of solid bioenergy carriers from biomass and waste. ECN-E-11-039.

Vollhardt, K.P.C., Schore, N.E., 2007. Organic Chemistry: Structure and Function. W. H. Freeman, New York.

Volpe, R., Messineo, A., Millan, M., Volpe, M., Kandiyoti, R., 2015. Assessment of olive wastes as energy source: pyrolysis, torrefaction and the key role of H loss in thermal breakdown. Energy 82, 119–127. https://doi.org/10.1016/j.energy.2015.01.011.

Wahid, F.R.A.A., Harun, N.H.H.M., Rashid, S.R.M., Samad, N.A.F.A., Saleh, S., 2017. Physicochemical property changes and volatile analysis for torrefaction of oil palm frond. Chem. Eng. Trans. 56, 199–204. https://doi.org/10.3303/CET1756034.

White, R.H., Dietenberger, M.A., 2001. Wood products: thermal degradation and fire. Encycl. Mater. Sci. Technol. 48, 9712–9716.

Wilk, M., Magdziarz, A., Kalemba, I., Gara, P., 2016. Carbonisation of wood residue into charcoal during low temperature process. Renew. Energy 85, 507–513. https://doi.org/10.1016/j.renene.2015.06.072.

Yuan, H., Wang, Y., Kobayashi, N., Zhao, D., Xing, S., 2015. Study of fuel properties of torrefied municipal solid waste. Energy Fuels 29, 4976–4980. https://doi.org/10.1021/ef502277u.

Yue, Y., Singh, H., Singh, B., Mani, S., 2017. Torrefaction of sorghum biomass to improve fuel properties. Bioresour. Technol. 232, 372–379. https://doi.org/10.1016/j.biortech.2017.02.060.

Zhang, C., Ho, S.H., Chen, W.H., Xie, Y., Liu, Z., Chang, J.S., 2018. Torrefaction performance and energy usage of biomass wastes and their correlations with torrefaction severity index. Appl. Energy 220, 598–604. https://doi.org/10.1016/j.apenergy.2018.03.129.